9th AUSTRALASIAN
FLUID MECHANICS CONFERENCE
AUCKLAND, 8-12 DECEMBER 1986

Unsteady Selective Withdrawal from a Line Sink

S. G. MONISMITH, J. IMBERGER[1] and G. BILLI

Centre for Water Research, University of Western Australia.
[1]On leave: Keck Laboratory, California Institute of Technology.

ABSTRACT

We present an experimental study examining the generation of internal waves by unsteady inertial outflows from a stratified reservoir. The experiments show that shear waves generated when the outflow is begun are identical to those generated when the outflow is stopped. The amplitudes of the lowest mode-number shear waves can be accurately calculated by assuming that they must combine to form the steady-withdrawal-layer velocity profile at the wall. As R, the parameter governing steady withdrawal behaviour, is increased, the observed shear wave amplitudes decrease relative to their theoretical values, with the discrepancy increasing with increasing mode number. When the outflow is repeatedly pulsed, the flow is generally directed towards the sink, suggesting that one effect of unsteady withdrawals may be to create a thicker effective withdrawal layer than would be found for similar steady withdrawals.

INTRODUCTION

The presence of a stable density stratification in storage reservoirs means that water withdrawn at a particular elevation tends to come primarily from adjacent strata. Information about selective withdrawal that is currently used by engineers in the design of offtakes has been mainly derived from experiments and theory concerned with withdrawal layer dynamics when the outflow is either steady, or is impulsively started and then allowed to run to a pseudo-steady state, i.e. a state in which the flow evolves over a period of time much longer than required for internal waves to actually set up the layer (Imberger, 1980). Thus we might ask: How should the steady theory be modified to account for the common case where the outflow rate varies considerably with time, i.e. what happens when the outflow changes before the steady layer has been established? To address this question, it is necessary to first consider how a steady withdrawal layer is set up.

When withdrawal of fluid from a stratified reservoir is suddenly started, the flow is initially potential (Pao and Kao, 1974; Imberger et al., 1976, hereafter ITF). The withdrawal layer first forms near the sink as buoyancy forces come into play, generating internal waves which modify the potential flow so that the velocity field away from the sink matches that at the sink (ITF).

The internal wave field so generated has a simple asymptotic form if the reservoir is much longer than it is deep (Pao and Kao, 1974). In this case non-hydrostatic pressures can be neglected; the resulting internal waves consist of an infinite series of columnar disturbances, called shear waves by McEwan and Baines (1974). Shear waves travel at the appropriate longwave speed; in a linearly stratified fluid of depth H, and buoyancy frequency, N, the n^{th} mode (one having n velocity nodes) travels at a speed, C_n, given by Pao and Kao (1974), as

$$C_n = NH(n\pi)^{-1} \quad . \tag{1}$$

Because of frequency dispersion due to non-hydrostatic effects, an initially sharp front diffuses; according to McEwan and Baines (1974), the frontal width S_n, defined as the distance over which the amplitude of the shear front changes from 10 to 90% of its full amplitude, at time T, asymptotically reaches the value (in a linearly stratified fluid):

$$S_n = H(NT)^{1/3} n^{-1} \quad . \tag{2}$$

Approximately 1/3 of the frontal region is ahead of the point where $n\pi X = NHT$, i.e. the position of the front neglecting dispersion. Finally, because of viscosity, shear wave amplitudes are attenuated with distance from the source of the waves; the e-folding time D_n is (Silvester, 1977; ITF)

$$D_n = 2\, n^{-2}\, \pi^{-2}\, \nu^{-1}\, H^2 \quad , \tag{3}$$

where ν is the kinematic viscosity of the fluid.

ITF developed a classification scheme, largely based on shear-wave dynamics, which showed that the evolution of the withdrawal flow is determined mainly by the value of the parameter R as defined by the relation

$$R = q(N\, \nu^2\, L^2)^{-1/3} \quad , \tag{4}$$

where q is the flow rate and L is the length of the reservoir. If R > 1, convection dominates and the shear waves will propagate out setting up an inertial withdrawal layer of thickness

$$\delta_I = O(q^{1/2}\, N^{-1/2}) \quad , \tag{5}$$

at a distance x from the sink in a time T_δ such that

$$NT_\delta = O(x\, \delta_I^{-1}) \quad . \tag{6}$$

Although there is some uncertainty for the case R > 1, the results of Silvester's (1977) experiments confirm much of ITF's analysis.

One obvious means of extending ITF's analysis to account for more general variations of flow rate with time is to suppose that the withdrawal layer is set up near the sink such that for any q, δ satisfies eq. 5. The resulting velocity distribution is then broken down into its modal components, which propagate as shear waves out into the interior of the fluid. This approach should be valid if the time required to establish the withdrawal layer near the sink, T_e, is much less than the time over which the flowrate varies. Since the region over which the isopycnals bounding the withdrawal layer are significantly drawn down has a width $O(\delta)$ (Pao and Kao, 1974; ITF), the fundamental setup time is $O(N^{-1})$, i.e. setting $x = \delta$ in eq. 6 gives $NT_e = 1$. Thus if $NT_f >> 1$, where T_f is the timescale of flow variations, the withdrawal layer thickness near the sink should satisfy eq. 5 as suggested. Where $x >> N\delta\, T_f$, the local flow will be determined by some superposition of decaying shear waves; consequently the local withdrawal layer may not satisfy eq. 5.

As part of a longer-term project investigating unsteady selective withdrawal, an experimental programme was designed to test this proposition for the simple case of a finite duration (pulse) outflow. The experimental results we present show that, with certain qualifications, this appears to be a valid approach to analysing the flow if R = O(1).

We will also present results from an experiment in which repeated opening and closing of the valve, and the consequent shear-wave generation led to a more complex velocity time series than was observed in single pulse experiments.

THEORY

As ITF's analysis shows, it is useful to study parts of the selective withdrawal flow in isolation. We will assume that the velocity distribution on the wall X = 0 (see Fig. 1) is known and examine the generation of shear waves by changes in that velocity distribution.

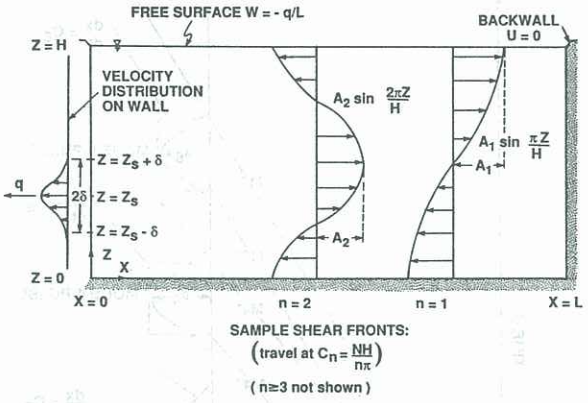

Fig. 1: Definition sketch for unsteady withdrawal from a stratified reservoir

Following ITF, using a balance of inertial and buoyancy forces we define non-dimensional variables as x = X/L, z = Z/H, T = T(NH/L), u = U/(q/H), and w = W/(q/H) (see Fig. 1). In the limit (λ = H/L, $F = q(NL^2)^{-1}$, $Gr^{-1} = N^2L^4\nu^{-2}$) all are infinite (ITF), the governing equations can be reduced (Gill and Clarke, 1974; Monismith, 1986) to the single pair of hyperbolic equations:

$$D_t\, u_n \pm c_n\, D_t\, \zeta_n = 0 \quad ; \qquad (7)$$

where the operator $D_t = (\partial_t \pm c_n \partial_x)$ is defined along characteristic curves in the (x,t) plane given by the relation

$$dx = \pm c_n\, dt \quad . \qquad (8)$$

The dimensionless velocity, u, and isopycnal displacement, $\partial_t \zeta = w$ (which replaces pressure) are given by the modal expansions (including the eigenfunctions appropriate to the case where N is a constant):

$$u = \sum_{n=1}^{n=\infty} u_n(x,t)(2^{1/2}n\pi\cos(n\pi z)) + u_0(x,t) \qquad (9)$$

and

$$\zeta = \sum_{n=1}^{n=\infty} \zeta_n(x,t)(2^{1/2}\sin(n\pi z)) \quad . \qquad (10)$$

We will not calculate u_0, the barotropic contribution to eq. 9 here because it does not directly affect the formation of the withdrawal layer (ITF); however, u_0, must be included so that the total velocity field can satisfy the free surface boundary condition shown in Fig. 1 (Gill and Clarke, 1974) since all of the baroclinic modes satisfy the condition w = 0 at the top and bottom of the water column. If u(x = 0,z,t) = f(z,t),

$$u_n(x = 0,t) = 2^{1/2}(n\pi)^{-1}\int_0^1 f(z,t)\cos(n\pi z)dz \quad . \qquad (11)$$

If the dimensionless height of the sink above the bottom is h, and we assume the distribution (Koh, 1966; Spigel and Farrant, 1984),

$$f(z,t) = (2\gamma)^{-1}[1 + \cos(\pi\gamma^{-1}(z - h))]\theta(t) \qquad (12)$$

for $z\varepsilon(h - \gamma, h + \gamma)$ and f(z,t) = 0 otherwise, where $\gamma(t) = (\delta/H)$ is the dimensionless withdrawal layer thickness (assuming that we know δ) and $\theta(t)$ is the fluctuating outflow rate (scaled by some mean value q), then $u_n(0,t)$ is easily evaluated by integrating eq. 11. The case γ = 0 was analysed by Pao and Kao (1974), ITF and Silvester (1977).

Once we know the initial conditions on u_n and ζ_n, and the boundary condition $u_n(0,t)$, we can integrate eq. 8 along characteristic curves given by eq. 9 to find the velocity field for all x (but not valid for x = O(λ)). For example if we suppose the $u_n(x,0) = \zeta_n(x,0) = 0$, then it can be shown that

$$u_n(x,t) = u_n(0,t - n\pi x) \quad , \qquad (13)$$

for an infinite duct, or for a finite reservoir before shear wave reflection. Fig. 2 sketches the situation for the case of a finite impulse, i.e. $\theta(t) = H(t) - H(t - t_{on})$, (H is the Heaviside step function) in a finite reservoir; in the absence of viscous dissipation, it is easy to see that the pattern $\theta(t)$ is repeated with a period of $2n\pi$. More general outflow patterns can be treated by simple means such as that discussed in Monismith (1985).

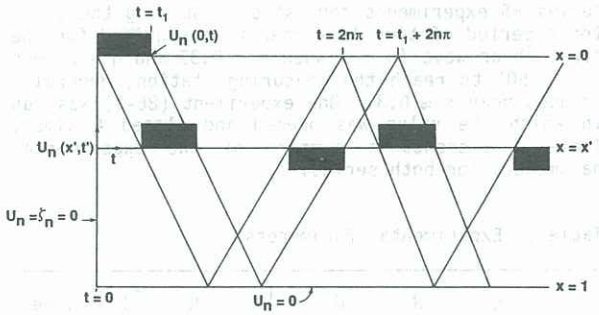

Fig. 2: Propagation of a modal pulse along characteristics in the (x,t) plane

Corrections for the effects of frequency dispersion, which mainly influence frontal width (McEwan and Baines, 1974; Pao and Kao, 1974), and dissipation (ITF), which reduces frontal amplitude, are relatively straightforward (c.f. eqs 1 and 2).

EXPERIMENTAL SETUP

Our experiments were performed in a tank 5500 mm long by 500 mm wide by 600 mm deep. Several 2 mm slits were machined in one end of the tank: the lowest slit, situated at z = 0, was used to fill the tank; the second slit, 155 mm off the bottom, was used to withdraw fluid from the tank. The fluid was linearly stratified with a mixture of salt and fresh water. The tank and filling process are described in detail in Silvester (1977). Density profiles were taken with conductivity probes mounted on stepper-motor-driven traverses.

Two means of measuring fluid velocity were used: the bead-plane technique developed by Silvester (1977), and a laser-Doppler anemomenter (LDA). The bead-plane technique was used in the first series of experiments (Exps 84-1, 84-2, and 84-3). This

technique entails photographing the motions of small, neutrally buoyant particles illuminated by a slit light source. Each exposure consists of three superposed images of the field particles, taken with short flashes at 4 sec. intervals. The velocity field within the camera's field of view is then derived for each exposure by measuring particle displacements. Silvester estimated that velocities measured with this technique are in error by no more than 0.01 mms^{-1}.

An LDA, set up in forward-scatter mode, was used in the second series of experiments (86-n) to measure the velocity at a fixed point in the tank (generally at $x \approx 0.3$, $z = h$). The LDA is made up of standard DANTEC 55x series optical components. On the receiving side, the photomultiplier-tube signal is fed into a frequency tracker where it is amplified and the Doppler signal extracted. The LDA's sensitivity, which is determined by the optical configuration, is 5.02 $MHz/(ms^{-1})$; consequently, the accuracy of the system as a whole is approximately 0.2 mms^{-1}. A digital representation of the Doppler frequency and an indication of tracker lock is sampled at 75 Hz by a microcomputer; all valid readings for a given 1 sec. interval are averaged together and stored. Because the flows were laminar, and because large density gradients were never created at the level of the measuring volume, signal dropout due to index-of-refraction variations was not a problem.

As we will discuss in the next section, the first series of experiments showed that the vertical structure of the shear wave modes was exactly as predicted theoretically (within experimental error); hence, in the second series of experiments, shear wave amplitudes were taken directly from the LDA measured velocities.

All of the series 84 experiments and most of the series 86 experiments consisted of opening the valve for a period of time less than that required for the first shear wave (n = 1 when h = 0.33 and n = 2 when h = 0.50) to reach the measuring station, generally located near $x \approx 0.3$. One experiment (86-5) was run in which the valve was opened and closed 4 times. Table 1 presents a summary of the experimental parameters for both series.

Table 1 Experimental Parameters

Exp.	q cm^2s^{-1}	N s^{-1}	H cm	T_{on} s	R	δ_I cm	Type
84-1	2.3	0.43	32.0	30	1.0	4.6	Bead/S
84-2	4.6	0.47	48.0	19	1.9	6.3	Bead/A
84-3	1.2	0.43	32.0	41	0.5	3.3	Bead/S
86-1	5.5	0.73	31.4	30	2.0	5.5	LDA/S
86-2	8.1	0.73	31.1	30	2.9	6.7	LDA/S
86-3	10.5	0.73	30.7	30	3.8	7.6	LDA/S
86-4	11.5	0.73	30.1	30	4.0	7.8	LDA/S
86-5	1.5	0.63	31.0	300	0.6	3.1	LDA/S

Note: 1. $\delta_I = 2.0\, q^{1/2}\, N^{-1/2}$.
2. Type refers to bead-plane vs. LDA velocity measurements; /S refers to symmetric withdrawal (h = 0.50) while /A refers to asymmetric withdrawal (h = 0.33).
3. 4 cycles, 300s on /300s off, in 86-5.

EXPERIMENTAL RESULTS

A potential flow was always set up by the propagation of a long surface wave when the valve was first opened; upon reflection from the far wall this wave developed into a barotropic seiche. This potential flow can fluctuate considerably if the valve is opened quickly; in particular, the unsteady barotropic (depth-averaged) velocity will be $O(q/H)$ which is comparable to the unsteady baroclinic velocity which is $U(q/\delta)$ since, $\delta = U(H)$ in our experiments. Because we are mainly interested in the baroclinic velocity field, the barotropic contribution to the measured velocity must somehow be removed. In the series 84 experiments, fluctuations in velocity due to the barotropic seiche were partially filtered out of the velocity measurements by the averaging inherent to the bead-plane technique. However, since the seiche period was roughly 6 sec. and the averages were over 8 sec., some additional error in measuring shear wave amplitudes may have been introduced. Barotropic motions were especially evident in preliminary runs made with the LDA; in the series 86 experiments the valve was opened slowly so as to eliminate the barotropic seiche as much as possible. By trial and error we found that if 5 sec. or more was taken to open or close the valve the amplitude of the barotropic seiche could be adequantely reduced.

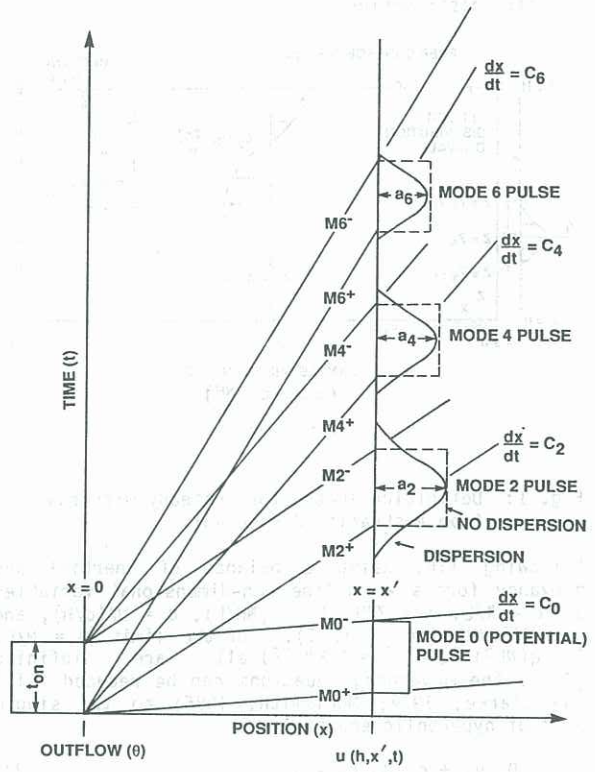

Fig. 3: A sketch showing the mode-number dispersive propagation of shear wave pairs in the x-t plane for the experimental conditions. M0 refers to the barotropic mode which propagates with dimensionless speed C_0. The effect of frequency dispersion on each of the pulses is also shown in approximate fashion

In the main group of experiments to be discussed (series 84 and 86-1 to 86-4) the outflow was stopped soon after it had been started. In all seven of these experiments, T_{on} was sufficiently small that none of the shear waves reached the measuring station before the valve was closed. These experiments proved ideal for examining shear wave propagation since in these experiments each of the first three (either n = 1,2,3 when h = 0.33, or n = 2,4,6 when h = 0.50) positive (generated by starting the flow) shear wave modes could be observed arriving at the measuring station, followed at the appropriate interval by its negative counterpart. Because of the difference in phase speed among the resulting modal pulses (see eq. 1), we observed each modal velocity distribution in isolation. This is sketched in Fig. 3. Each positive wave set up the

appropriate velocity profile; subsequently, each negative wave returned the velocity profile to one showing no motion. This is shown clearly in Fig. 4 which plots velocity profiles at three different times in Exp. 84-3. The shape of each profile is very close to the modal form, $u \sim \cos(n\pi z)$.

The departure at any given time of the shear wave fronts from their step function shape in the x direction because of frequency dispersion can be seen in Fig. 5a-5c, which plots the spatial structure of modes 2,4, and 6 in Exp. 84-3, at the time(s) they were within the camera's field of view. Because of the isolation of each mode, and because only even modes are present, centreline velocities are equivalent to modal amplitudes. The positions of the fronts, as calculated using Eq. 1, ($n\pi$ x = t) are also marked in each figure.

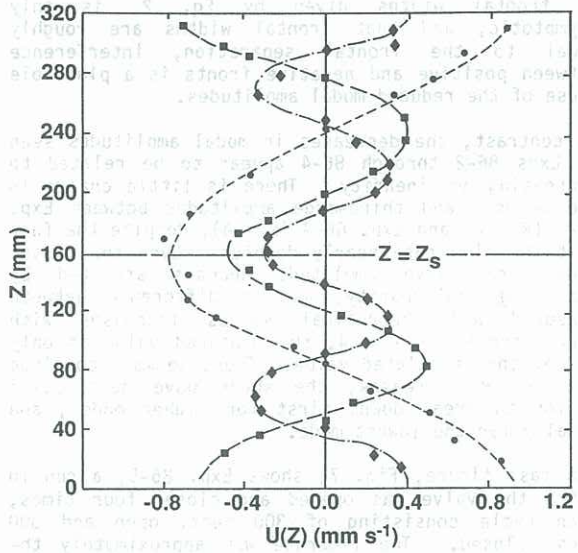

Fig. 4: Velocity distributions in exp. 84-3: (●) mode 2 at (X,T)=(193cm,110s); (■) mode 4 at (X,T)=(161cm,170s); (▲) mode 6 at (X,T)=(174cm,274s)

The temporal evolution of the centreline velocity at a fixed x position can be seen in Fig. 6a-6c, which plots LDA-measured velocities as functions of time in Exps 86-1, 86-2, and 86-4. Experiments 86-1 through 86-4 were all performed without refilling the tank after the first experiment in the group since the changes in fluid depth induced by the short outflows (T_{on} = 30 sec.) were quite small (approximately 2% of the depth between Exps 86-1 and 86-2); essentially the only parameter which differs among these four experiments is q, the outflow rate. All four of these experiments have values of R > 1, and show the effect on the flow of increasing R, i.e. increasing nonlinearity, while keeping all the other parameters more-or-less fixed.

Figure 6a-6c shows the same isolation of shear wave modes seen in the series 84 experiments. The leading and trailing edges of the pulses shown in Fig. 6 correspond quite well to the calculated arrival times of pairs of positive and negative shear waves; accordingly, we have only indicated on Fig. 6 which mode, e,g. mode-2 (M2) is responsible for a particular pulse in the velocity signal. Figure 6a is the clearest in showing the potential flow, four pairs of outgoing shear wave modes (n = 2,4,6 and 8), and several reflections of the mode-2 pulse. Although the other two plots are similar, as R is increased (Fig. 6b and 6c), first-mode shear wave amplitudes increase proportionately more that do those of the higher modes. In Fig. 6b, the mode-8 pulse is virtually nonexistent. In spite of a 50% increase in flow rate between Exps 86-1 and 86-2, the amplitudes of the mode-4 and mode-6 pulses in Exp. 86-2 are only marginally larger than those seen in Exp. 86-1. This trend of relative reductions in higher mode amplitude continues a R is increased: in Fig. 6c, the only identifiable modal pulse is the mode-2 pulse.

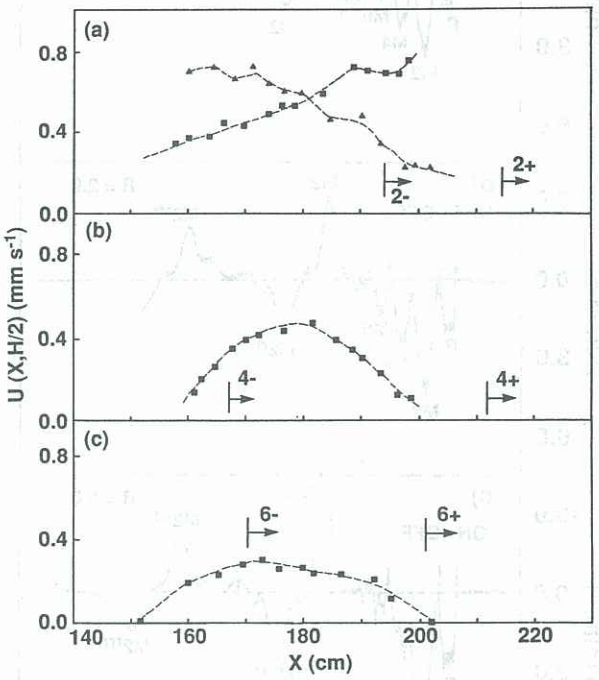

Fig. 5: Horizontal distribution of centreline velocity in exp. 84-3: (a) mode 2 at t = 98s (▲) and t = 130s (■); (b) mode 4 at t = 194s; (c) mode 6 at t = 274s

A further important difference between Fig. 6a (or 6b) and 6c is the appearance of short period (roughly 20 sec.) waves following the mode-2 pulse. Dyestreaks near the sink indicated that motions of fluid in the withdrawal layer towards the sink continued after the valve was closed (this is to be expected, according to linear theory). As this flowing layer collided with the wall, a series of bulges, similar in appearance to the solitary waves observed by Kao and Pao (1980), developed and propagated into the interior of the fluid. We speculate that these 'solitary' waves are the short period waves seen in Fig. 6c.

From Fig. 5a-5c, Fig. 6a-6c, and similar figures for the other series 84 (see Billi, 1984) and series 86 experiments we have estimated the modal amplitudes for the first three modal pulses. We have then compared them with theoretical values calculated according to the theory presented in Section 2 and using a numerical integration of Eq. 11, assuming that $\delta_I = 2.0(q/N)^{1/2}$ (Imberger, 1980), and accounting for viscous dissipation using Eq. 3. The results are presented in Table 2, which shows a reasonably good agreement between theory and observations. The results for Exps 84-1, 84-3, and 86-1 agree most closely with theory; in these three cases, the difference between theory and observation is within the expected experimental error ~ 0.1 mms^{-1} - mainly due to surface seiching). It should be noted that the assumption that δ is finite gives second and third-mode amplitudes 20 to 30% smaller than the values calculated assuming that δ = 0.

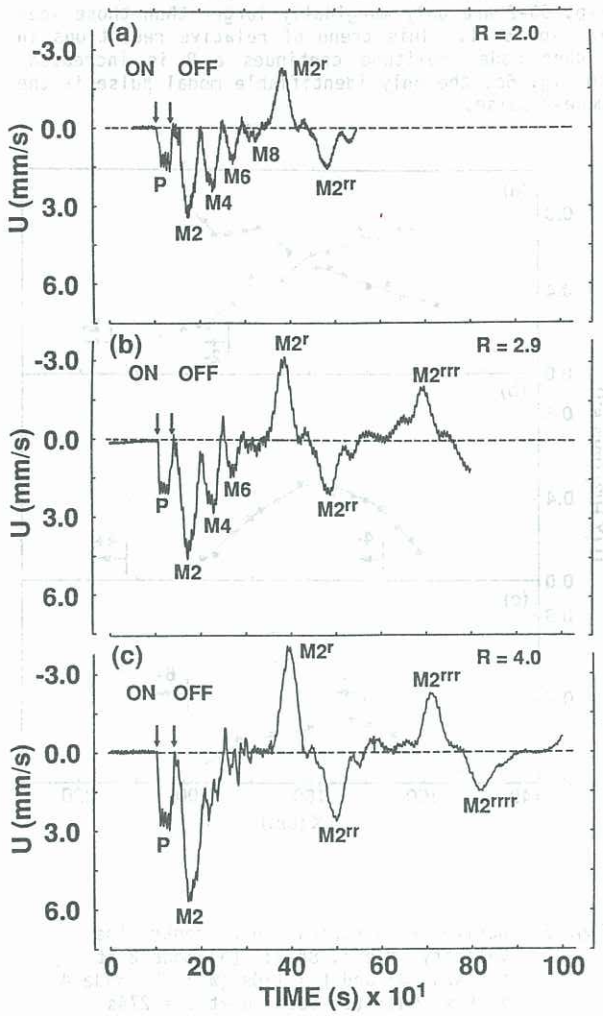

Fig. 6: Velocity time series in (a) exp. 86-1, (b) exp. 86-2, and (c) exp. 86-3. Positive velocity means flow towards sink. Mn refers to the mode-n pulse, while the superscript r refers to the number of reflections

Table 2 Modal Amplitudes

Exp.	R	γ	a_1 (mms^{-1}) meas.	a_1 (mms^{-1}) theory	a_2 (mms^{-1}) meas.	a_2 (mms^{-1}) theory	a_3 (mms^{-1}) meas.	a_3 (mms^{-1}) theory
84-1	1.0	0.14	1.20	1.38	0.75	0.98	0.45	0.51
84-2	1.9	0.13	0.90	0.95	0.67	0.91	0.80	1.72
84-3	0.5	0.10	0.80	0.74	0.55	0.61	0.35	0.37
86-1	2.0	0.18	3.15	3.22	2.12	2.30	1.06	1.20
86-2	2.9	0.22	4.09	4.60	2.37	2.98	1.13	1.24
86-3	3.8	0.25	4.84	5.78	2.21	3.31	0.96	1.04
86-4	4.0	0.25	5.38	6.52	1.53	3.73	-	1.40

Note: 1. $\gamma = \delta_I H^{-1}$.
2. All theoretical values calculated according to Eq. 11, including the viscous correction to amplitude, Eq. 2.
3. For Exp.84-2 h = 0.33 all other experiments h = 0.50, for this h = 0.33 subscripts 1, 2 and 3 refer to n = 1,2,3 otherwise to n = 2,4, and 6.
4. Measured mode-2 amplitude in Exp. 86-4 is questionable, see Fig. 5c.

In the other three experiments, the difference between theoretical and measuring values increases with increasing mode number. There appear to be at least two possible sources for this effect: nonlinearity and frontal interference. Consider first Exp. 84-2, which exhibits the largest discrepancies between theory and observation in the 84 series and which was the shortest run of the series (T_{on} = 19 sec.). This experiment was carried out at R = 1.9, roughly the same value of R as in Exp. 86-1, in which there was found good agreement between measured and calculated modal amplitudes. This rules out nonlinearity as the primary cause. Next consider the effects of the short outflow time. We calculate that the shear fronts should have had the following separations between positive and negative fronts: (n = 1) 136 cm, (n = 2) 68 cm, (n = 3) 45 cm. When the measurements were made, the frontal widths should have been 123 cm, 68 cm and 52 cm respectively. Considering that the estimate of frontal widths given by Eq. 2, is only asymptotic, and that frontal widths are roughly equal to the frontal separation, interference between positive and negative fronts is a plausible cause of the reduced modal amplitudes.

In contrast, the decreases in modal amplitudes seen in Exps 86-2 through 86-4 appear to be related to increasing nonlinearity. There is little change in the second- and third-mode amplitudes between Exp. 86-2 (R = 2) and Exp. 86-4 (R = 4), despite the fact that the flow rate nearly doubles. Even the first-mode shear wave amplitude appears affected by inceasing nonlinearity, as the difference between measured and theoretical values increases with increasing R; at R = 4, the measured value is only 83% of the calculated value. Thus, we must conclude that as R increases, the shear wave description begins to break down, first for higher modes, and finally for the lowest mode.

The last figure, Fig. 7, shows Exp. 86-5, a run in which the valve was opened and closed four times, each cycle consisting of 300 secs. open and 300 secs. closed. The flowrate was approximately the same for each of the four pulses. Using the initial value of N and the average value of q, the time to steady-state $T_\delta = 4X(N\delta)^{-1}$ (the constant of proportionality in Eq. 6 is taken from Ivey and Blake, 1985), is calculated to have been 350 secs.

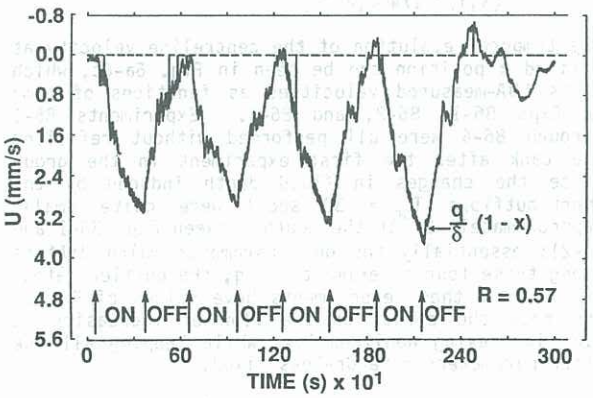

Fig. 7: Velocity time series in exp. 86-5

Two aspects of Fig. 7 are of particular interest: (1) the amplitude of the velocity pulse measured in the interior grows with time, and (2) the flow is almost entirely towards the sink. The growth in pulse amplitude indicates that each set of positive and negative shear waves generated after the first set was able to add to the amplitude of the previous positive and negative fronts. The observation that the flow was almost always forward was supported by observations of the deformation of dyestreaks in the tank. As in Silvester's (1977) experiments,

initially vertical dyestreaks showed the sequence of arrivals of shear waves. However, the dyestreaks also showed a net deformation between the beginning and end of an experiment at elevations above and below the boundaries of the steady withdrawal layer. Because of the decay of higher-mode motions, the forward flow at the measuring stations was dominated by lowest-mode motions; hence the effective withdrawal layer at the measuring station was thicker than the withdrawal layer near the sink itself.

CONCLUSIONS

While it is well known that waves can be generated by starting to withdraw fluid from a stratified reservoir, experiments and theory presented in this paper show that negative waves of equal amplitude can be generated when withdrawal is stopped. A finite pulse outflow will result in a pair of shear waves propagating through the fluid such that the modal component of the pulse travels at the appropriate modal speed. The amplitudes of the few lowest-mode pulses can be calculated with reasonable accuracy by assuming that the velocity distribution at the wall is the steady withdrawal profile given in eq. 12.

As suggested by ITF, the number of wave modes whose behaviour can be described by the linear theory decreases with increasing value of the parameter R. At the highest value of R attained in this study, only the lowest-mode pulse was observed. Furthermore, the amplitudes of high-mode waves appear to depend on the length of time flow is maintained; for very short outflow pulses, the discrepancy between theoretical and observed modal amplitudes increased with increasing mode number.

One noteworthy feature of the multiple pulse experiment that was carried out was that the flow at the point of measurement was always towards the sink. Since this sinkward flow was primarily caused by the passage of lowest mode shear waves, the effective withdrawal layer, in terms of overall changes in the density stratification, may have been much thicker than the steady withdrawal layer set up near the sink.

ACKNOWLEDGEMENTS

This work was supported by the Western Australian Water Authority as part of the CWR-WAWA Canning project and by the Australian Research Grants Scheme. Technical assistance for the project was provided by the Department of Civil Engineering at the University of Western Australia and by the Centre for Environmental Fluid Dynamics. In particular, we wish to thank Dr B. Coghlan of the CEFD for writing data acquisition software for the LDA. The second author thanks the Fairchild Fellowship program at the California Institute of Technology for financial support.

REFERENCES

Billi, G (1984): Unsteady selective withdrawal from a line sink. Honours thesis, University of Western Australia.

Gill, A E; Clarke, A J (1974): Wind-induced upwelling, coastal currents and sea-level changes. Deep Sea Reseach, vol. 21, 325-345.

Imberger, J (1980): Selective withdrawal: a review. IAHR Proc. Second International Symposium on Stratified Flows, Trondheim, Norway, vol. 1, 381-400.

Imberger, J; Thompson, R O R Y; Fandry, C (1975): Selective withdrawal from a finite rectangular tank. J. Fluid Mechanics, vol. 70, 489-512.

Ivey, G N; Blake, S (1985): Axisymmetric withdrawal and inflow in a density-stratified container. J. Fluid Mechanics, vol. 161, 115-137.

Kao, T W; Pao, H P (1980): Wake collapse in the thermocline and internal solitary waves. J. Fluid Mechanics, vol. 97, 115-127.

Koh, R C Y (1966): Viscous stratified flow towards a sink. J. Fluid Mechanics, vol. 24, 555-575.

McEwan, A D; Baines, P G (1974): Shear fronts and an experimental stratified shear flow. J. Fluid Mechanics, vol. 65, 657-688.

Monismith, S G (1985): Wind induced motions in stratified lakes and their effect on mixed-layer shear. Limnology and Oceanography, vol. 30, 771-783.

Monismith, S G (1986): The modal response of reservoirs to wind stress. J. Hydraulics Division of the ASCE, (submitted to).

Pao, H P; Kao, T W (1974): Dynamics of establishment of selective withdrawal of a stratified fluid from a line sink. Part 1. Theory. J. Fluid Mechanics, vol. 65, 657-688.

Silvester, R (1978): An experimental study of end wall effects on selective withdrawal from a reservoir. Ph.D thesis, University of Western Australia.

Spigel, R H; Farrant, B (1984): Selective withdrawal through a point sink and pycnocline formation in a linearly stratified flow. J. Hydraulic Research, vol. 22, 35-51.